The Flight Performance of the Galileo Orbiter USO[1]

D. D. Morabito
Telecommunications Systems Section

T. P. Krisher
Navigation Systems Section

S. W. Asmar
Telecommunications Systems Section

Results are presented in this article from an analysis of radio metric data received by the DSN stations from the Galileo spacecraft using an Ultrastable Oscillator (USO) as a signal source. These results allow the health and performance of the Galileo USO to be evaluated, and are used to calibrate this Radio Science instrument and the data acquired for Radio Science experiments such as the Redshift Observation, Solar Conjunction, and Jovian occultations. Estimates for the USO-referenced spacecraft-transmitted frequency and frequency stability have been made for 82 data acquisition passes conducted between launch (October 1989) and November 1991. Analyses of the spacecraft-transmitted frequencies show that the USO is behaving as expected. The USO was powered off and then back on in August 1991 with no adverse effect on its performance. The frequency stabilities measured by Allan deviation are consistent with expected values due to thermal wideband noise and the USO itself at the appropriate time intervals. The Galileo USO appears to be healthy and functioning normally in a reasonable manner.

I. Introduction

This is an article on the efforts to characterize the instrument used for the Galileo Radio Science investigation. It discusses the performance of the USO, which, when the spacecraft and ground elements of the instrument are configured in the one-way mode, is the limiting error source observed in the received Doppler data at time intervals where there is sufficient signal power.

Galileo was originally scheduled to be launched in May 1986, but was delayed due to the Challenger accident. Galileo was launched on October 18, 1989, and on December 5, 1989, the USO was turned on. Galileo acquired gravity assists from Venus (February 1990) and Earth (December 1990, December 1992) and will go into orbit around Jupiter in December 1995. Between December 1989 and November 1991, 94 one-way passes were scheduled for 2-hr data acquisition periods. However, not all scheduled passes resulted in valid data; twelve passes were lost for various reasons (six were aborted after a spacecraft safing anomaly early in 1990, four were lost due to a crashed se-

[1]Due to an error in the production of *The Telecommunications and Data Acquisition Progress Report 42-113*, this article is being reprinted in its entirety.

quence in March–April 1991, and two were lost due to tape problems). Data for the remaining 82 passes were acquired by the DSN and delivered to the Galileo Radio Science Team (RST) for analysis in the form of Archival Tracking Data File (ATDF) tapes. Estimates of the spacecraft-transmitted frequency and frequency stability were made for the 82 passes conducted during these first two years of cruise. Each pass consists of about 2 hr of Doppler data sampled at 1/sec, and hydrogen masers served as the frequency and timing references. The received Doppler data were converted into estimates of spacecraft-transmitted frequencies and frequency residuals after accounting for spacecraft trajectory and other effects.

II. Purpose

The USO-referenced data were acquired for two purposes: (1) the scientific investigation of the redshift phenomenon, which is the frequency shift as the spacecraft moves in and out of the gravitational fields of massive bodies in the solar system as predicted by Einstein's theory of general relativity, and (2) the engineering evaluation of the USO frequency and frequency stability for calibration purposes and to evaluate the health and performance of the USO. These calibration data serve as a baseline for Radio Science experiments such as the Redshift Observation, Solar Corona Experiment, and occultations of Jupiter and its satellites. This article will focus only on the engineering aspects of the USO data. The scientific results are discussed in [1]. For discussions of the expected scientific results of the Galileo Radio Science investigations, the reader is referred to [2,3].

The goal of the USO analysis is thus to establish the USO-referenced spacecraft-transmitted frequency and the frequency stability associated with it, as well as phase noise and spectral purity (when using open-loop data) and to build a database containing the statistics and all parameters relevant to the measurements.

III. Spacecraft Configuration

The Galileo spacecraft configuration for these Radio Science tests is the normal cruise configuration, with the exception of a "TWNC-ON" command which enables the USO to be the radio downlink reference; this is the mode required for the redshift experiment and future occultation investigations. No other changes (e.g., a modulation index change) were requested for this purpose. The majority of the tests were performed on a quiet spacecraft where no maneuvers or other motion were permitted to occur.

The USO, a science payload instrument integrated with the spacecraft's telecommunications subsystem, was manufactured by Frequency Electronics Inc., New York, between 1975 and 1976. The USO which resides in the Radio Frequency Subsystem (RFS) of the Galileo orbiter is serial number 4, from the same lot as the USO's flown on Voyagers 1 and 2. The Voyager 1 USO failed in November 1992 (after 15 yr of continuous service), engendering concerns about the survival lifetime of the Galileo USO. The USO is a dual-oven–controlled device with an AT-cut quartz-crystal (SiO_2) resonator. The design output frequency is 19.125000 MHz corresponding to channel 14. When the USO is the downlink signal source, it drives the 2.3-GHz exciter. The output frequency is multiplied in the transponder by a factor of 120 to produce the 2.3-GHz transmitted signal (~2294.9976 MHz). The 2.3-GHz Traveling Wave Tube Amplifier (TWTA) amplifies the signal it receives from the 2.3-GHz exciter to either one of two power levels: the high-power mode (27 W) or the low-power mode (9 W). The TWTA has routinely been configured to the high-power mode. The 2.3-GHz TWTA provides the amplified RF output to the High-Gain Antenna (HGA)/Low-Gain Antenna (LGA) transmit switch of the 2.3-GHz antenna switch, which connects the outputs of the 2.3-GHz TWTA's to either the HGA or the LGA. If the HGA is ever successfully deployed, an 8.4-GHz transmitted signal will also become available and will be 11/3 of the 2.3-GHz signal frequency.

All of the data acquired were at 2.3 GHz and right circularly polarized. The signal was transmitted from the spacecraft via either LGA-1 or LGA-2. LGA-1 is located on the spacecraft spin-axis in front of the HGA tip sunshade. LGA-2 is located on a boom 3.58 m away from the spin axis, and is pointed in the direction opposite that of HGA and LGA-1. Both LGAs work at 2.3 GHz only. LGA-2 was utilized for the period right after launch and the period right after the Earth 1 encounter. The time periods of the spacecraft LGA configuration for the data set analyzed in this article are:

10/18/89 to 03/15/90	LGA-2
03/15/90 to 12/08/90	LGA-1
12/08/90 to 01/31/91	LGA-2
01/31/91 to 11/30/91	LGA-1

The Galileo spacecraft is a spin-stabilized spacecraft which rotates at about 3 rpm.

IV. Ground Data System Configuration

The DSN configuration was that of normal cruise tracking with the addition of the Radio Science subsystem to acquire open-loop data for certain passes. The radio metric data were sampled at a rate of 1/sec using a loop filter bandwidth of 10 Hz. For all of the passes, hydrogen masers were the frequency and timing references at the ground stations. The overall stability of the ground system (frequency reference, receiver, cables, etc.) is expected to be at about 1×10^{-15} at 1000 sec, which is far more stable than the USO.

The open-loop receiver utilized a 100-Hz bandwidth filter and a sampling rate of 200 per sec. Data were recorded on 1600-bpi or 6250-bpi Original Data Record (ODR) tapes which were delivered to the Galileo RST.

V. Data Products

The following data products are received for each pass assuming they were requested and no failures occurred: (1) an ATDF tape containing the closed-loop Doppler data, (2) an ODR tape containing the open-loop data records (when applicable), (3) a pass folder from the DSN containing copies of frequency predictions, operator logs and related material, and (4) a spacecraft trajectory vector file from the Galileo Navigation group. References on interface agreements and software interface specifications for the data products are available from the Radio Science System's Group Library. The data products are received, logged, validated (tapes only), and archived by the Radio Science Data Production System.

VI. Analysis Software and Techniques

The analysis was performed on the Radio Science Support System Radio Occultation Data Analysis Network (RODAN) computer which includes a Prime 4050 computer, a Floating Point Systems (FPS) array processor, two magnetic tape drives and other peripherals. The system is accessible by a set of IBM PS/2 terminals as well as two Sun workstations.

Although the analysis tools used for this work were inherited from the Voyager Project, there were enough differences in configuration and procedures in the Galileo Project that nontrivial modifications were made to the software and the techniques. The analysis software was upgraded to estimate more accurately the spacecraft-transmitted frequency and the frequency residuals used for the stability analysis, including installation of code to model the effects introduced by a spinning spacecraft.

The data were processed by the STBLTY software program set. Figure 1 is a block diagram displaying the interconnection of the component programs with the various input data types, intermediate files, and output files. The functions of each of the component programs are described below.

PLLDEC: If open-loop data are to be processed, the phase-lock-loop program PLLDEC is utilized to perform signal detection on the digitized open-loop samples read from the input ODR or Intermediate Data Record (IDR) tapes. The detected frequencies and time tags are written to an output file (F36), and the open-loop receiver tuning (POCA) frequencies are written to a separate file (F33).

OCEP: In the case of closed-loop data, OCEP reads the Doppler counts and Doppler extractor reference frequency from an input ATDF tape, converts these to sky frequencies, and writes the time-tagged sky-frequency data and related information to the F50 disk file. In the case of open-loop data, OCEP reads the PLLDEC output files (F36, F33), converts to sky frequencies and writes the time tags, sky frequencies and other related information to the F50 disk file.

GETTRAJ: Reads the spacecraft state vectors from the Navigation Team–provided Celestial Reference Set (CRS) file, performs vector manipulations and light-time solutions, and writes a disk file (F45) containing the time-tagged spacecraft position and velocity vectors relative to the Sun and the observing DSN station. Details of the orbit-determination solutions determined by Galileo navigation used to generate the trajectory files are given elsewhere [4].

RESID: Reads the sky frequencies from the OCEP output file (F50), and the trajectory vectors from the GETTRAJ output file (F45). Model downlink sky frequencies are estimated from the trajectory vectors, and are corrected for troposphere, spacecraft spin, gravitational redshift and, if applicable, the spinning off-axis LGA-2–induced Doppler signature. RESID estimates the spacecraft-transmitted frequency at the time tag of the first data point, and computes the frequency residuals by differencing the observed sky frequencies from the estimated sky frequencies for each data point. The troposphere model is a simple zenith path delay translated

to the line-of-sight elevation angle. A spacecraft spin model correction is applied to the estimated downlink frequency and residuals. The magnitude of this correction depends upon whether the spacecraft was in all-spin mode (0.0481 Hz) or dual-spin mode (0.0525 Hz). The sign of this correction depends upon whether the signal source was LGA-1 or LGA-2. RESID writes the residual frequencies and related information to the F52 output file.

Relativistic effects, including the gravitational redshift, are modeled in the analysis, and removed from the data. The results of the scientific analysis of these effects, the first test of the solar redshift with an interplanetary spacecraft, indicate that the total frequency variation as predicted by general relativity has been verified to an accuracy of 0.5 percent and the solar gravitational redshift to 1 percent [1]. Therefore, it can be stated with a reasonable degree of confidence that the redshift effect is removed to the stated accuracy.

STBLTY: Reads the RESID output file (F52), computes and applies a bias correction to the spacecraft-transmitted-frequency estimate relative to the center of weight of the residuals over the pass, and computes phase, Allan variance, frequency and phase power spectral densities (PSD's), and other relevant statistics, and writes the relevant information for the current pass to a database summary file. STBLTY also produces plots of relevant data quantities.

Once all of the USO passes have been processed through the above programs, the database file will contain a set of records for each processed pass. This file is then processed through the following two programs:

FITUSO: Reads the USO frequencies from the database, and fits and removes an aging model. The resulting post-fit residuals are written to a previously blank field in the database. The user can specify how many passes to skip, how many passes to accept and where the break between logarithmic and linear aging behavior occurs.

USOSMRY: Reads the USO database and displays graphically any requested quantities from a menu of available data types.

VII. Analysis Results

A. General Single Pass Results

Of 94 scheduled USO-referenced data acquisition passes, 82 were processed through the STBLTY program set. Each pass was typically 2 hr in duration. All data processed were closed-loop data acquired by the Deep Space Stations (DSS's) sampled at 1/sec. Table 1 displays the year, day number, UTC start time, UTC end time, DSS station identification, signal level (AGC), and estimated spacecraft-transmitted frequency for each pass. Figure 2 displays a typical plot of the residuals after the removal of the spacecraft trajectory, the gravitational redshift, a simple troposphere model, and the effect of the spacecraft spin when LGA-1 is the signal source. Figure 3 displays the frequency residuals after every 60 points have been averaged, allowing long-period trends to be examined easily. Figure 4 displays the reconstructed phase for the residuals of Fig. 2. Figure 5 is the log of the Allan deviation for the residuals of Fig. 2. Figures 6 and 7 display the logs of the frequency spectral density and phase spectral density, respectively, for the residuals of Fig. 2. The spikes at about 0.05 Hz are related to the 3-rpm spacecraft spin.

B. LGA-2–Induced Spin Doppler Example

When LGA-2 is the signal source, there is a significant sinusoidal signature present in the received Doppler due to LGA-2 being mounted on a boom located 3.58 m from the spacecraft spin axis. Figure 8 displays a typical plot of frequency residuals for a pass where LGA-2 was used, after the trajectory and other effects were removed. Figure 9 clearly illustrates the sinusoidal signature for a selected 200-sec period.

In order to remove this signature from the data, a three-parameter sinusoidal model was iteratively fit to the Doppler residuals of Fig. 8. This model includes an amplitude, a frequency and a phase offset. After the model was successfully fit and removed, the resulting post-fit residuals (see Fig. 10) yielded Allan deviations consistent with those of LGA-1 passes, suggesting that the three-parameter sinusoidal model is sufficient for removal of the spin-induced Doppler signature.

For three passes where LGA-2 was the signal source, 91-01-14 (91-014), 90-01-09 (90-009) and 90-12-10 (90-345), dynamic activity occurred on board the spacecraft which introduced phase shifts into the data. The result is that the fit of the sinusoidal model failed to remove all of the induced off-axis LGA-2 Doppler signature, resulting in residuals as exemplified in Fig. 11 for pass 91-014. In this specific case, tape-recorder motion was known to occur, where the envelope changes in Fig. 11 correlate with the tape-recorder start and stop times. Figure 12 illustrates the resulting degradation to the Allan deviation (compare with Fig. 5). Pass 90-345 occurred after the Earth 1 flyby where several activities occurred on board

the spacecraft which introduced dynamic motion. Stator prepositioning commands introduced dynamic motion on the spacecraft during the data acquisition period for pass 90-009. In these cases, the dynamic activity was assumed to be symmetric about the center of weight of the spacecraft and thus appeared not to have biased the estimated spacecraft-transmitted frequencies which are determined at the first data point, and then corrected to the center of weight of the full data span. The Allan deviations for these passes were, however, degraded.

C. Solar Interference Example

Figure 13 displays the residuals for pass 91-03-05 (91-064) where several solar disturbances occurred during that day including the period of the data acquisition. The degradations in the observed Doppler noise measurements from the closed-loop system are consistent with those expected from solar interference.[1] This was the only pass in this data set where this behavior was observed. The estimated spacecraft-transmitted frequency appears reasonable; however, the Allan deviations were degraded as expected.

D. Stability Analysis Results

The Allan deviation is the recommended measure of oscillator stability for time-domain signal processing. For all 82 passes, the Allan deviations are displayed in Figs. 14–17 for 1-, 10-, 100- and 1000-sec time intervals, respectively. Outlier points are annotated with the year and day number of the pass (YR-DOY). Note that outlier points are especially apparent for time intervals of 10, 100 and 1000 sec. These include (1) the three LGA-2 passes, 900109 (90-009), 901210 (90-345), and 910114 (91-014), where dynamic events occurred on the spacecraft, (2) the suspected solar interference pass, 910305 (91-064), (3) three passes, 900330 (90-089), 911019 (91-292) and 911130 (91-334), where the cause of the degradation is not known, but is possibly due to ground equipment problems, and (4) the first two passes after initial turn-on, 89-341 and 89-350, where the significant increasing frequency dynamics adversely dominated the Allan deviation measurements at 1000 sec (see Fig. 17).

When the outlier passes are removed, the resulting Allan deviation plots for the remaining passes at 1-, 10-, 100- and 1000-sec time intervals are displayed in Figs. 18–21, respectively.

The measured means and errors of the Allan deviations are given in Table 2 for each time interval (outlier passes were removed as well as three passes where the data were insufficient to estimate Allan deviations at 1000 sec). The pre-flight Allan deviation measurements of the Galileo USO for these time intervals are also presented in Table 2.[2] The pre-flight measurements were performed at the JPL Hydrogen Maser Test Facility on May 1, 1980. Figure 22 is a plot of the measured flight Allan deviation averages with the complete set of pre-flight measurements superimposed.

For 1 and 10 sec, the flight-measured Allan deviations significantly exceed the pre-flight Allan deviations. This was expected since it is known that wideband thermal system noise (white phase noise) dominates at these time intervals due to the low signal-to-noise ratios resulting from using Galileo's low-gain antennas. The flight-measured Allan deviations agree with estimates derived from the measured signal levels, system noise temperatures and receiver bandwidths. The Allan deviations at 1 sec (Fig. 18) and 10 sec (Fig. 19) also correlate with spacecraft range (compare with Fig. 23). If the HGA ever becomes available, and if there is an opportunity to turn off the telemetry modulation to increase the signal strength, there will be better visibility of the true USO performance at the 1-sec and 10-sec time intervals.

The flight-measured Allan deviations at 100 and 1000 sec agree well with the corresponding pre-flight values in Table 2 and Fig. 22. This implies that the flight data are dominated by the true behavior of the USO at these time intervals. The hump at 70 sec in the pre-flight values in Fig. 22 has been attributed to the thermal oscillation of the inner oven current driven by noise.[3] The consistent behavior of the flight data between 100 and 1000 sec with the pre-flight measurements at these time intervals implies that this effect is visible in the flight data. In the absence of this thermal cycling, one would then expect the Allan deviation behavior to be flat over these time scales, and thus be consistent with flicker frequency noise. The expected noise due to unmodeled media fluctuations lies well below this level at these time intervals.

The Allan deviation behavior for the flight data measurements can be broken down into several regions. The

[1] R. Woo, personal communication, Radio Frequency and Microwave Subsystems Section, Jet Propulsion Laboratory, Pasadena, California, August 1992.

[2] A. Kirk, "Frequency Stability Measurements of Galileo Project High Stability Crystal Oscillators," JPL 331-TRAK-800527 (internal document), Jet Propulsion Laboratory, Pasadena, California, May 1, 1980.

[3] G. E. Wood, personal communication, Telecommunications Systems Section, Jet Propulsion Laboratory, Pasadena, California, February 1993.

Allan deviation in the 1- to 10-sec region falls roughly as τ^{-1}, characteristic of white phase noise dominating at these time intervals. The USO behavior here is masked by this noise at these time scales. The behavior of the region from 100 to 1000 sec can be interpreted as being consistent with the known inner-oven thermal cycling effect being superimposed on a flicker frequency noise floor (using the pre-flight measurement information). Between 1000 sec to about 40,000 sec, one can assume a continuation of the flicker noise floor upon inspection of the pre-flight measurements and error bars. The 17-mHz rms scatter of the estimated flight frequencies about an aging model (see Section VII.F) is consistent with the random walk inferred by extrapolating the pre-flight Allan deviation measurements as $\tau^{1/2}$ to a weekly time interval, but could include some unknown mismodeling.

E. Signal Levels

The USO passes have relatively low signal levels as exhibited in the plot of spacecraft signal levels (AGC) of Fig. 24. The observed values of the Allan deviations at small time intervals are consistent with those derived for thermal noise theory using measurements of system noise temperature and the measured signal levels presented in this plot. The AGC correlates well with spacecraft range (Fig. 23).

After correcting the received signal levels displayed in Fig. 24 for receiver station antenna gain, space loss, spacecraft LGA antenna gain, and telemetry state carrier suppression, the resulting spacecraft-transmitted 2.3-GHz power levels at the RFS/antenna subsystem interface of the spacecraft were computed. The 42.2-dBm mean value of the LGA-2 passes was in good agreement with the expected power level, while the 40.0-dBm mean value for the LGA-1 passes was about 2 dB lower than the expected power level.[4] The resulting rms scatters of about 2 dB were consistent with the known calibration uncertainties at the ground stations.

F. Analysis of Spacecraft-Transmitted Frequency Measurements

The frequency transmitted by the spacecraft was estimated for all 82 passes. Figure 25 displays the USO-referenced spacecraft-transmitted frequencies as estimated by STBLTY. Each point on the plot is the USO frequency estimated at the first time tag for that pass and then corrected to the center of weight of all of the residuals over that pass. The assigned uncertainties of the estimated frequencies run about 3 mHz and are dominated by the uncertainty inferred from not performing an ionospheric correction. The plot is annotated with the times the USO was powered on and off. The time axis is in days since January 1, 1989. The USO was initially powered on in flight on December 5, 1989 (DOY 339). There was one instance of cycling the USO off (91-217) and then back on (91-228) in this data set.

A preliminary pass of a few minutes' duration was conducted shortly after initial turn-on on December 5, 1989 (and after the inter-oven current was allowed to stabilize), in order to verify operation of the USO. Here the frequency was observed to be increasing at a very high rate and exhibited dynamic behavior due to early impurity migration and/or stress relief resulting in the very poor stability expected shortly after turn-on. The first valid USO pass was conducted on December 7, 1989, several hours after initial turn-on.

Changes in the USO frequency with time are referred to as resonator aging. In general, the principal causes of aging are stress relief in the mounting structure of the crystal unit, mass transfer to or from the resonator's surface due to adsorption or desorption of contamination, changes in the oscillator circuitry, and possibly changes in the quartz [5]. Aging effects seen in this data set likely include surface liberation of impurities, impurity migration across and within the crystal, and linear aging (diffusion). The significant positive logarithmic increase in frequency shortly after initial turn-on (see Fig. 25) is probably due to the liberation of contamination on the crystal resonator surfaces which were acquired during the long period of inoperation prior to launch.[5] The USO was powered off for much of the time that the spacecraft was dormant on the ground prior to launch (1986–1989). The linear region is expected to be reached after the USO has been turned on for a sufficiently long enough period of time such that the only significant aging mechanism is diffusion. The curvature observed for the 6 passes conducted after the USO was cycled off and back on in August 1991 could be attributed to stress relief and migration of impurities.

During the first USO-on cycle (December 1989 to August 1991), 76 passes of USO data were acquired. Each pass consisted of about 2 hr of 1/sec sampled Doppler

[4] A. Makovsky, *Galileo Orbiter Functional Requirements,* module *Galileo Orbiter Telecommunications Functional Requirement Document,* JPL Document 625-205, 3-300B (internal document), Jet Propulsion Laboratory, Pasadena, California, May 9, 1989.

[5] R. L. Sydnor, personal communication, Communications Systems Research Section, Jet Propulsion Laboratory, Pasadena, California, September 3, 1992.

(Fig. 26). An aging model was removed from the estimated spacecraft-transmitted frequencies for this period so that the resulting residuals could be analyzed and remaining error sources identified. The model removed was of a combination logarithmic curve and a linear aging drift:

$$\hat{f}_{s/c} = C_1 \log_e [C_2 (t - t_0) + 1] + C_3 + C_4 (t - t_0) \quad \text{for } t < t_b$$

$$\hat{f}_{s/c} = C_5 + C_6 (t - t_b) \quad \text{for } t \geq t_b$$

where t_0 is the time tag of the first data point, and t_b is the time tag of the first data point of where the linear aging realm begins. C_1 through C_6 are constant coefficients, which were estimated by least-squares analysis.

The initial attempt to fit this model over the data acquired during the first USO-on cycle resulted in the residuals displayed in Fig. 27. A large systematic variation is evident for passes occurring shortly after the USO was powered on, suggesting that the model is insufficient for this period. The rms scatter of the residuals is about 48 mHz with a χ_n^2 of 272. Since the behavior of the USO is known to be complex during this period and not easily modeled (initial stabilization phenomena mask the aging behavior), the first 12 passes were deleted, and the model was fit to the remaining 64 passes (see Fig. 28). The corresponding post-fit residual plot of Fig. 29 displays significantly less scatter and no significant systematic variation. The rms residual scatter of this fit was 17 mHz with a χ_n^2 of 35. It is believed that the 17-mHz variations are due to the random walk of the USO or mismodeling. In an attempt to identify any mismodeling, the post-fit residuals were examined against troposphere correction, spacecraft–Earth–Sun angle, elevation angle, spacecraft range, signal level (AGC), gravitational redshift correction, station identification, USO oven current (from telemetry), and spacecraft temperatures (from telemetry). No apparent correlations or trends were detected. The observed 17-mHz scatter is consistent with random walk behavior, as discussed previously (see Section VII.D).

The logarithmic time constant C_2^{-1} was estimated to be about 71 days. The turnover of the curve occurred 259 days after initial turn-on. The slope of the linear aging region was estimated to be -1.50×10^{-7} Hz/sec, which is in agreement with the measured slope of the Voyager 2 USO (-1.28×10^{-7} Hz/sec).[6] This translates to an aging rate over a 1-day period of -5.6×10^{-12}, which shows that the USO is drifting well below its specification of 5×10^{-11}/day.[7]

In an attempt to verify when the USO had reached its linear aging realm, different subsets of the last several passes in Fig. 28 were subjected to linear fits of frequency versus time. Initial fits of the last 31 passes prior to first turn-off (90-262 to 91-154), and the last 21 passes (90-360 to 91-154) displayed a signature in the residuals with significant curvature. A linear fit of the last 19 passes (91-006 to 91-154) showed no significant residual signature and yielded results consistent with the logarithmic and linear combination fit discussed previously. This implies that the Galileo USO required a little over a year of operation time prior to reaching its linear aging realm.

It is preferred that once the USO is switched on, it is left on so that it is allowed to reach the linear aging realm where it should remain for the duration of the Galileo activities. The linear aging realm allows one-way Radio Science experiments, such as the gravitational redshift experiment and planetary occultations, to be accurately calibrated. Since August 1991, the USO was switched off and back on in support of cooling turns as part of the effort to free the HGA stuck ribs (in conjunction with corresponding warming turns). The USO and its heater were powered off on August 5, 1991 (91-217). There were 6 passes conducted after the USO was powered back on August 16, 1991 (91-228). The estimated spacecraft-transmitted frequencies for these passes display a smooth continuity in time (see Fig. 30). A simple four-parameter aging model was fit to these frequencies yielding a post-fit rms scatter of 3 mHz. Although the number of points and the time period were insufficient to infer an accurate linear aging rate, this result suggests that the USO is behaving in a reasonable manner during this period. The USO was again turned off after this time period. If the USO had been allowed to remain on, it was expected that not as long of a period would be required for it to reach its linear aging realm as it did during the first on–off data set (89-341 to 91-154). The Allan deviations appear consistent with those of the first on–off data set, although two of the passes have somewhat higher values.

G. Retrace

If the USO and its heater are turned off, and then turned back on, the crystal will oscillate at a different frequency which is difficult to predict. This phenomenon

[6] S. W. Asmar, and P. M. Eshe, "Evaluation of the USO Performance - Final Report," JPL IOM Voyager-RSST-90-121 (internal document), Jet Propulsion Laboratory, Pasadena, California, January 17, 1990.

[7] A. Gussner, "Summary of Galileo USO Testing," JPL IOM 3364-80-080 (internal document), Jet Propulsion Laboratory, Pasadena, California, August 20, 1980.

known as retrace is defined as the nonrepeatability of the frequency versus temperature characteristic at a fixed temperature upon on–off cycling of the oscillator [5]. An example of retrace is the 12-Hz jump between passes on 91-154 and 91-247 (see Fig. 25). Between these passes, the USO and its oven were turned off for an 11-day period in August 1991. Several mechanisms which can cause retrace include strain changes, changes in the quartz, oscillator circuitry changes, contamination redistribution in the crystal enclosure and apparent hysteresis [5].

H. Assessment of Environmental Effects

The frequency of the USO can change due to variations in environmental parameters which include temperature, pressure, acceleration, magnetic field, and radiation. The crystal frequency is also dependent on the power level. Discussions are presented in [5–7] on the effects of the various phenomena on the behavior of crystal oscillator devices.

The Galileo USO was designed to minimize the effects of magnetic fields. A worst-case estimate of the magnetic field of the spacecraft in the environment of the USO found that the resulting fluctuations in frequency were expected to be negligible for the 10- to 1000-sec time intervals.[8]

Since the USO is oven-controlled so as to maintain a constant temperature, and the crystal temperature is designed to operate at an optimum point on the f versus T curve, noise due to temperature fluctuations is expected to be insignificant.

The majority of the USO passes were conducted during quiescent periods on the spacecraft when there was no scheduled dynamic activity. The few known exceptions of dynamic activity involved no net thrusts on the spacecraft. Acceleration effects on the spacecraft USO are considered to be negligible.

It is assumed that in the deep space environment, changes due to atmospheric pressure and humidity are virtually nonexistent. Pre-launch testing showed that the Galileo USO exhibited spikes of less than 1 mHz during changes in pressure.[9]

Due to the high level of shielding, no charged particles are expected to hit the crystal during cruise. High-energy particles are expected to be stopped by the lead shielding, producing photons which could possibly hit the crystal.[10] The level of radiation reaching the crystal during the cruise phase is expected to cause negligible shifts in frequency. The USO frequency could, however, shift about 1 Hz during passage through the Jovian radiation belts.[11]

VIII. Conclusion

The Galileo USO appears to be healthy and functioning in a reasonable manner based on the analysis presented in this article. The evaluation of the Radio Science instrument will continue for the duration of the Galileo radio propagation investigations.

[8] R. Postal, "A Concern of USO Stability as a Function of Magnetic Field," JPL IOM 3362-87,019 (internal document), Jet Propulsion Laboratory, Pasadena, California, June 3, 1987.

[9] A. Gussner, "Summary of Galileo Ultra Stable Oscillator (USO) Testing," JPL IOM 3364-80-080 (internal document), Jet Propulsion Laboratory, Pasadena, California, August 20, 1980.

[10] G. E. Wood, personal communication, Telecommunications Systems Section, Jet Propulsion Laboratory, Pasadena, California, February 1993.

[11] G. E. Wood, "Radiation Testing of Ultra Stable Oscillator S/N 004," JPL IOM 3396-76-095 (internal document), Jet Propulsion Laboratory, Pasadena, California, August 20, 1976.

Acknowledgments

P. Eshe, R. Herrera and T. Horton of the Radio Science Support Team provided valuable support. The comments and discussions provided by R. Sydnor and G. Wood, and R. Filler of LABCOM, New Jersey, were greatly appreciated. We acknowledge assistance by the Galileo Flight Team and the Galileo Navigation Team. The Deep Space Network generated the data. The authors thank W. Mayo of the Galileo Telecom Team for providing USO oven current and spacecraft temperatures.

References

[1] T. P. Krisher, D. D. Morabito, and J. D. Anderson, "The Galileo Solar Redshift Experiment," *Physical Review Letters*, vol. 70, pp. 2213–2216, April 12, 1993.

[2] H. T. Howard, V. R. Eshleman, D. P. Hinson, A. J. Kliore, G. F. Lindal, R. Woo, M. K. Bird, H. Volland, P. Edenhofer, M. Pätzold, and H. Porsche, "Galileo Radio Science Investigations," *Space Science Reviews*, vol. 60, pp. 565–590, 1992.

[3] J. D. Anderson, J. W. Armstrong, J. K. Campbell, F. B. Estabrook, T. P. Krisher, and E. L. Lau, "Gravitation and Celestial Mechanics Investigations with Galileo," *Space Science Reviews*, vol. 60, pp. 591–610, 1992.

[4] V. M. Pollmeier and P. H. Kallemeyn, "Galileo Orbit Determination from Launch through the First Earth Flyby," *Proceedings of the 47th Ann. Meeting of the Inst. of Nav.*, Williamsburg, Virginia, pp. 9–16, June 10–12, 1991.

[5] J. R. Vig, *Introduction to Quartz Frequency Standards*, Research and Development Technical Report SLCET-TR-92-1 (Rev. 1), Army Research Laboratory, Electronics and Power Sources Directorate, Fort Monmouth, New Jersey, October 1992.

[6] D. P. Howe, *Frequency Domain Stability Measurement*, National Bureau of Standards, Technical Note 679, U.S. Department of Commerce, PB-252-171, Washington, D.C., March 1976.

[7] B. Parzen, *Design of Crystal and Other Harmonic Oscillators*, New York: John Wiley and Sons, 1983.

Table 1. Galileo USO pass summary.

Year	DOY	Start hr:min:sec	End hr:min:sec	DSS id.	AGC, dBm	(Spacecraft-Transmitted Frequency − 2294997000), Hz
89	341	21:34:22	23:27:59	14	−149.5	690.321
89	350	00:02:40	01:57:59	14	−142.4	696.287
89	360	22:35:42	00:00:59	14	−145.5	699.954
90	2	17:09:45	18:59:59	14	−149.0	701.425
90	9	17:37:22	19:26:08	14	−149.6	702.669
90	15	17:34:22	19:28:11	14	−153.1	703.597
90	19	16:10:46	17:57:50	14	−156.1	704.134
90	28	16:00:09	18:00:00	14	−154.3	705.128
90	32	15:33:51	17:29:59	14	−155.8	705.508
90	37	10:50:57	12:12:36	63	−155.0	705.895
90	44	03:00:00	05:19:59	43	−151.6	706.383
90	46	00:19:29	01:04:57	43	−154.3	706.523
90	49	19:44:31	21:22:29	43	−153.9	706.855
90	56	02:10:12	03:26:48	43	−157.4	707.295
90	58	23:08:28	01:01:01	43	−158.5	707.457
90	61	00:17:51	01:55:53	43	−162.2	707.586
90	68	02:12:12	03:42:02	43	−159.5	707.987
90	76	02:19:06	03:28:03	43	−165.0	708.376
90	78	00:41:32	02:27:47	43	−166.5	708.452
90	83	19:13:51	20:56:11	43	−167.5	708.708
90	89	00:09:38	02:03:16	43	−166.8	708.888
90	97	22:18:28	23:55:22	43	−165.3	709.205
90	104	22:14:52	23:56:39	43	−167.6	709.422
90	110	00:47:05	02:26:45	43	−168.0	709.570
90	113	20:46:51	22:01:00	43	−169.0	709.671
90	121	23:21:02	00:57:56	43	−166.5	709.875
90	128	09:26:40	11:04:42	63	−168.3	710.014
90	136	23:22:03	01:16:30	43	−167.0	710.111
90	139	19:55:00	21:48:51	43	−166.9	710.166
90	149	19:17:45	21:02:08	43	−165.0	710.337
90	155	19:18:09	19:45:01	43	−165.7	710.395
90	162	18:14:46	19:43:47	14	−166.6	710.457
90	172	15:18:15	17:04:29	14	−164.8	710.566
90	176	16:19:35	18:05:46	14	−165.7	710.587
90	183	18:20:15	20:07:25	43	−165.6	710.634
90	193	14:48:37	16:34:51	14	−162.8	710.704
90	197	18:19:45	20:02:33	43	−165.0	710.720
90	206	21:17:32	23:00:05	43	−165.3	710.737
90	213	21:12:49	22:03:33	43	−165.6	710.769
90	221	20:43:23	22:29:37	43	−163.7	710.778
90	228	18:14:37	19:59:44	43	−162.8	710.775
90	233	15:17:38	17:03:53	14	−168.1	710.785
90	243	19:44:31	21:24:40	43	−165.5	710.764
90	250	01:41:02	02:45:10	63	−162.7	710.757
90	253	19:13:26	20:55:34	43	−161.1	710.735

Table 1. (cont'd).

Year	DOY	Start hr:min:sec	End hr:min:sec	DSS id.	AGC, dBm	(Spacecraft-Transmitted Frequency − 2294997000), Hz
90	262	19:26:55	21:11:16	43	−160.5	710.731
90	268	00:30:00	03:40:00	63	−162.5	710.706
90	274	18:56:25	20:43:34	43	−160.1	710.658
90	281	17:12:34	18:54:36	43	−156.9	710.612
90	303	01:44:22	03:23:19	63	−153.0	710.495
90	312	01:16:55	02:57:56	63	−148.5	710.432
90	321	03:18:28	04:58:11	63	−145.1	710.326
90	330	01:13:20	02:57:56	63	−145.0	710.271
90	345	02:14:52	03:42:02	42	−138.4	710.169
90	350	08:18:28	10:12:02	61	−147.7	710.115
90	360	17:09:14	18:57:41	43	−150.3	709.991
91	4	07:32:13	07:49:48	63	−149.4	709.922
91	6	18:01:47	19:58:45	43	−149.1	709.885
91	14	16:55:11	18:46:30	43	−152.5	709.792
91	16	17:04:22	18:59:59	43	−151.3	709.769
91	19	16:05:14	17:59:59	43	−152.5	709.743
91	21	18:04:52	19:58:57	43	−153.1	709.709
91	26	16:07:05	17:50:51	43	−154.8	709.657
91	29	06:07:42	07:58:54	63	−156.1	709.638
91	33	15:58:12	17:43:56	43	−158.1	709.577
91	36	06:07:11	07:58:50	63	−162.6	709.548
91	39	06:05:08	08:01:13	63	−160.9	709.507
91	43	15:05:08	16:59:59	43	−162.2	709.459
91	49	21:21:14	23:13:13	43	−160.6	709.370
91	55	15:35:23	17:30:30	43	−160.7	709.300
91	64	14:05:14	16:02:30	43	−158.6	709.173
91	73	16:23:17	18:13:59	43	−160.2	709.068
91	81	15:08:37	17:02:30	43	−155.4	708.929
91	109	19:02:38	20:45:14	43	−155.4	708.563
91	141	00:02:40	01:59:52	63	−157.6	708.161
91	154	23:04:06	00:59:41	61	−164.6	707.997
91	247	16:39:14	18:23:50	63	−167.5	696.304
91	259	21:28:12	23:11:46	14	−164.8	696.556
91	275	00:59:23	02:43:34	43	−165.9	696.678
91	292	15:15:11	17:00:01	63	−168.2	696.728
91	318	03:54:25	05:29:56	43	−168.1	696.772
91	334	20:41:17	22:10:45	14	−165.9	696.769

Table 2. Summary of Galileo USO Allan deviations.

Time interval, sec	Measured flight $\times 10^{12}$	Measured pre-launch $\times 10^{12}$
1	29.4 ± 1.1	0.56
10	3.93 ± 0.17	0.56
100	0.90 ± 0.03	1.1
1000	0.71 ± 0.03	0.68

Note: Uncertainties are errors in the mean.

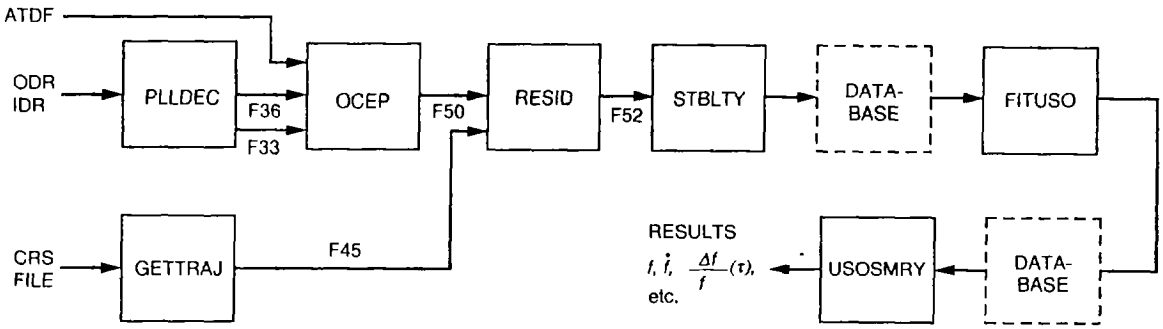

Fig. 1. STBLTY program-set block diagram.

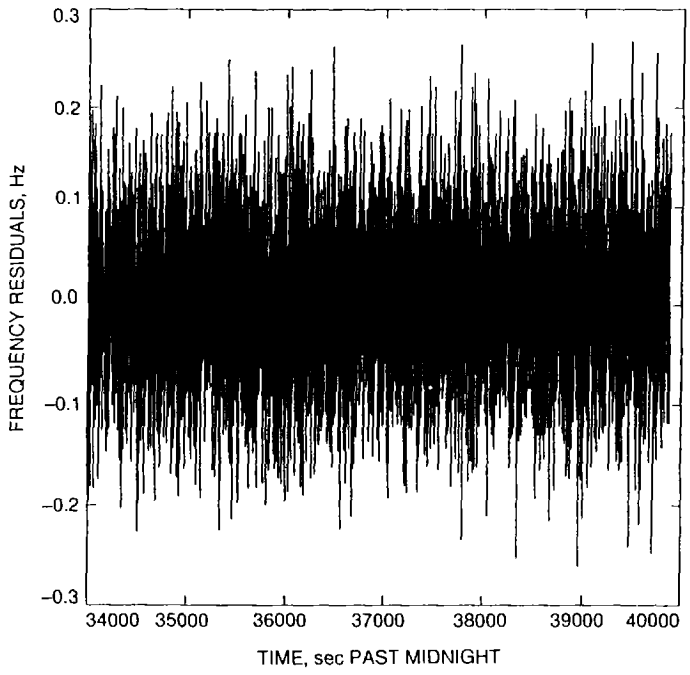

Fig. 2. Frequency residuals of sampled 1/sec Doppler for the USO pass of May 8, 1990.

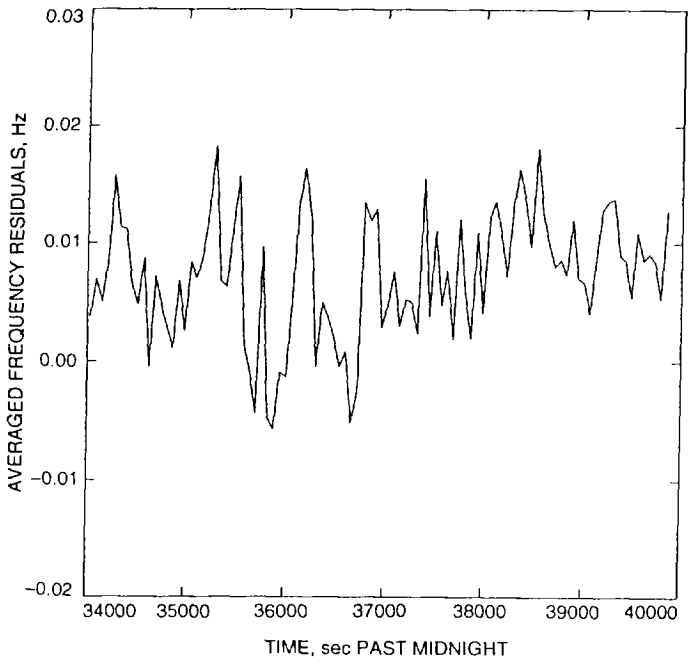

Fig. 3. Frequency residuals averaged every 60 sec for the USO pass of May 8, 1990.

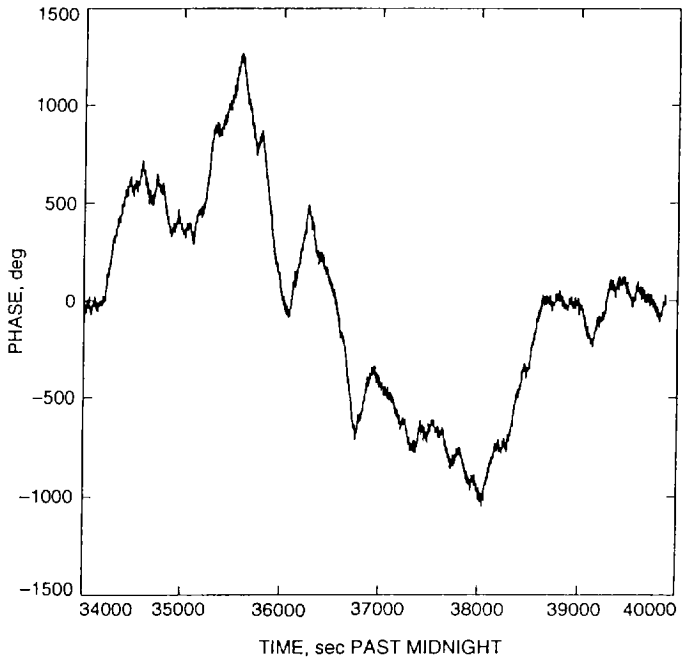

Fig. 4. Phase reconstructed from frequency residuals for the USO pass of May 8, 1990.

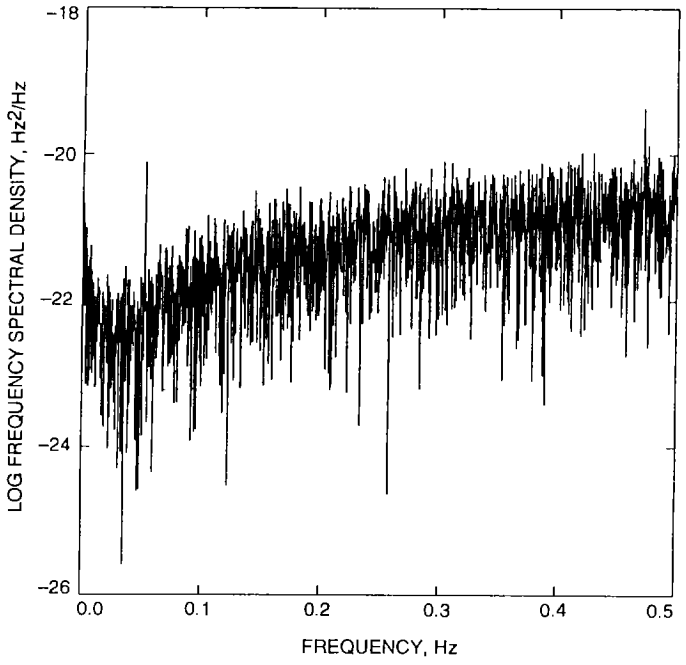

Fig. 6. Log of frequency spectral density of frequency residuals for the USO pass of May 8, 1990.

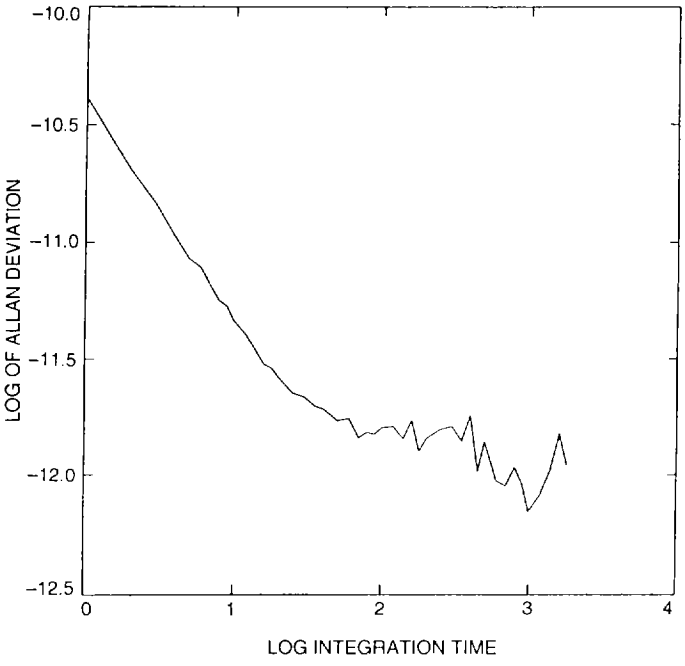

Fig. 5. Log of Allan deviation of frequency residuals for the USO pass of May 8, 1990.

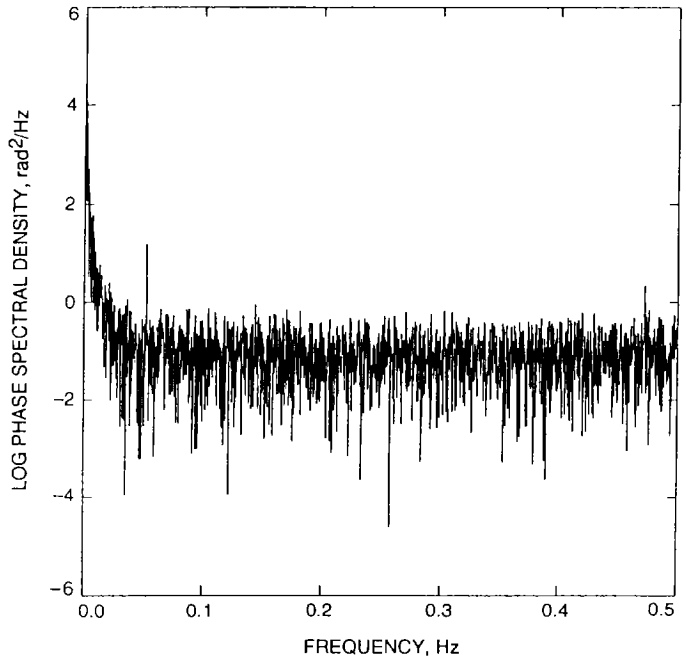

Fig. 7. Log of phase spectral density of frequency residuals for the USO pass of May 8, 1990.

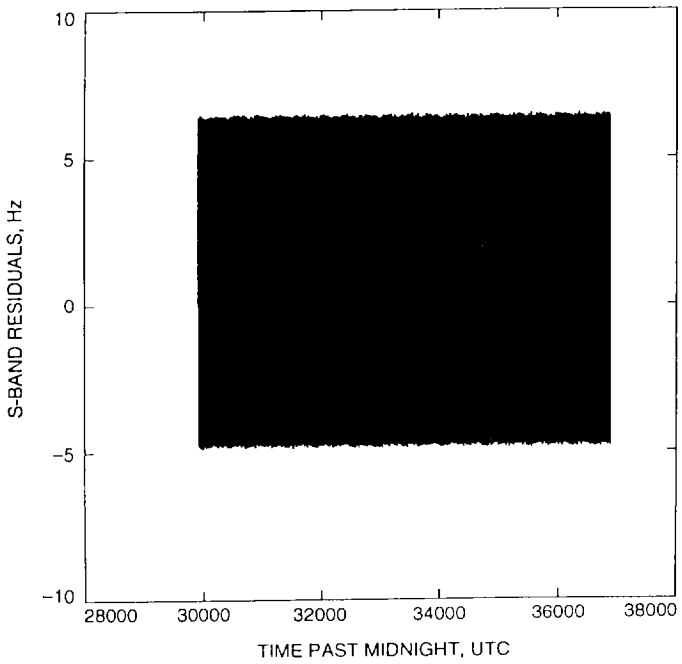

Fig. 8. Frequency residuals of sampled 1/sec Doppler for USO pass of December 16, 1990, where LGA-2 was the spacecraft antenna.

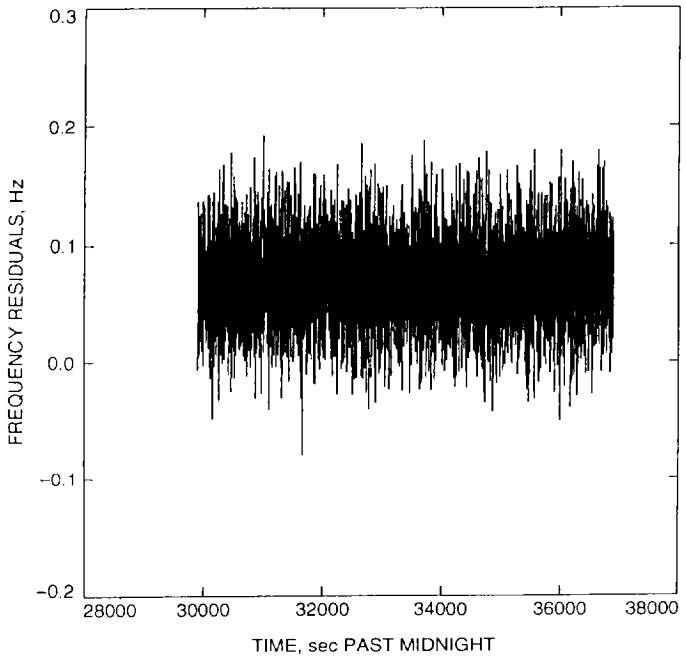

Fig. 10. Frequency residuals after removing the sinusoid fit from residuals displayed in Fig. 8 for USO pass of December 16, 1990, where LGA-2 was the spacecraft antenna.

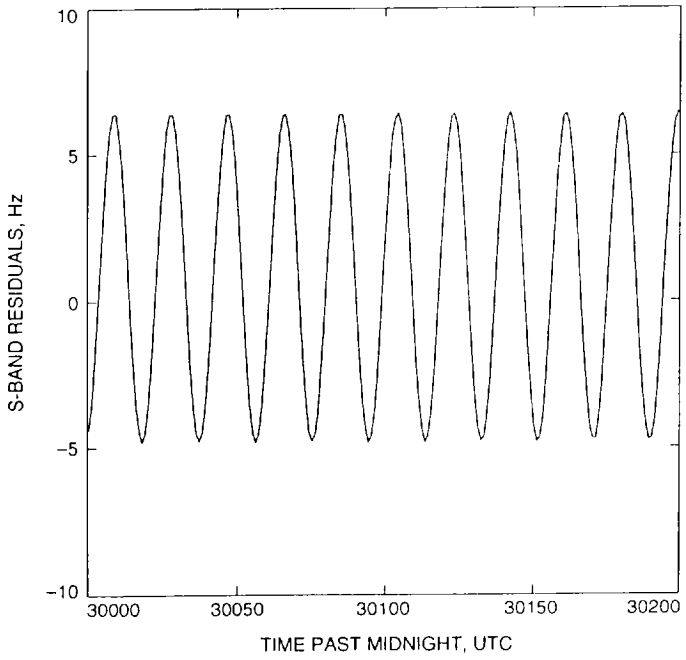

Fig. 9. Selected 200-sec period of frequency residuals of sampled 1/sec Doppler for USO pass of December 16, 1990, where LGA-2 was the spacecraft antenna.

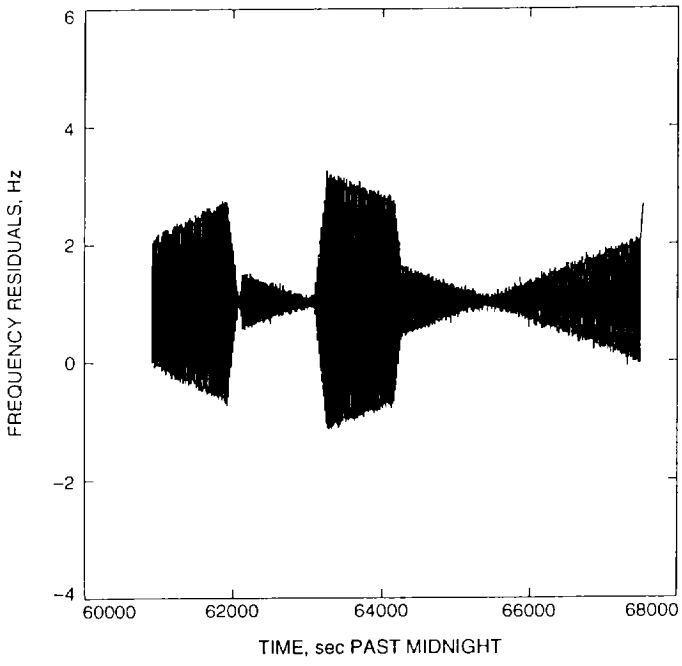

Fig. 11. Frequency residuals of sampled 1/sec Doppler for the USO pass of January 14, 1991, where LGA-2 was the signal source and dynamic motion occurred on board the spacecraft.

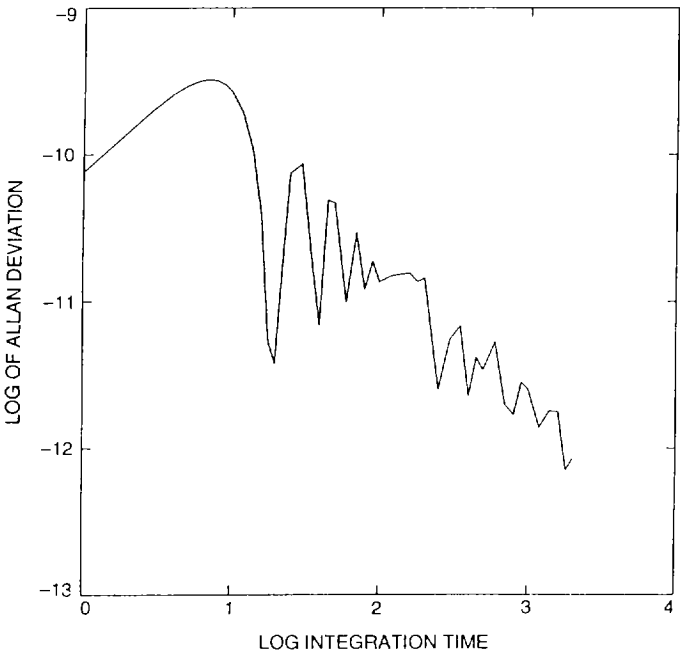

Fig. 12. Log of Allan deviation of frequency residuals of Fig. 11.

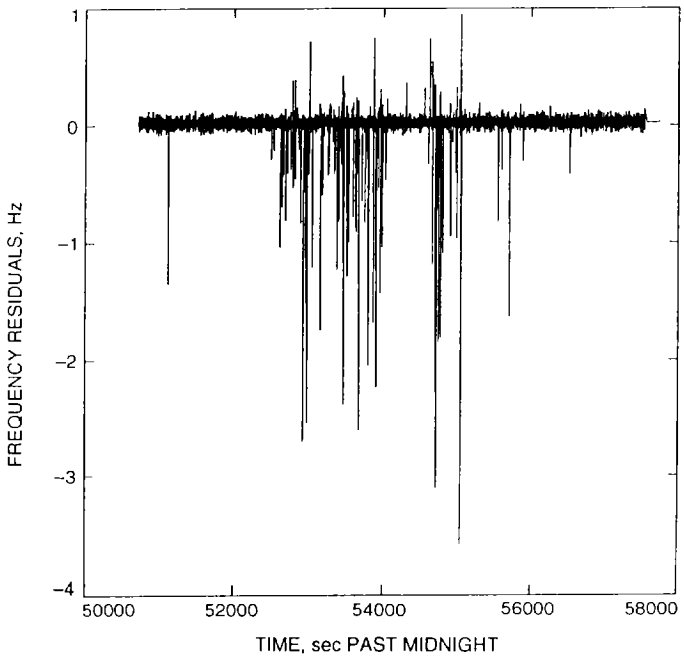

Fig. 13. Frequency residuals of the USO pass of March 5, 1991, where solar activity was known to have occurred.

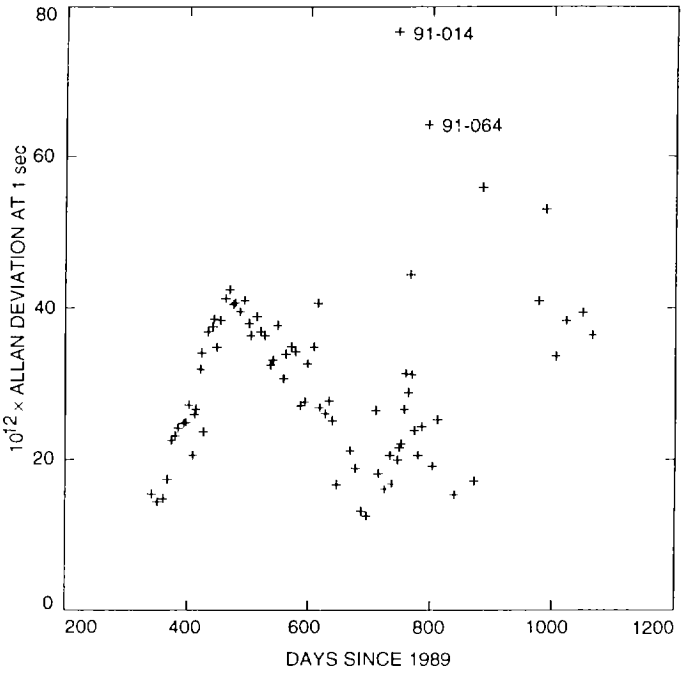

Fig. 14. Allan deviations at 1 sec for the 82 USO passes.

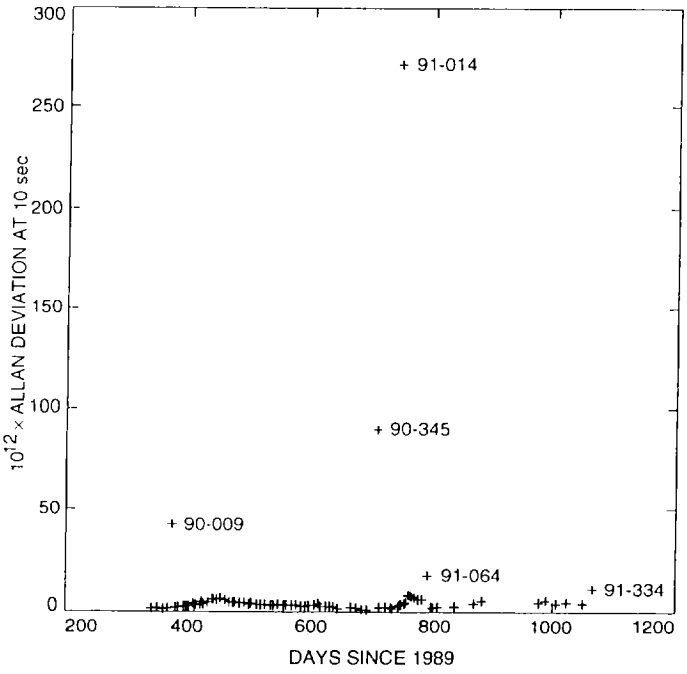

Fig. 15. Allan deviations at 10 sec for the 82 USO passes.

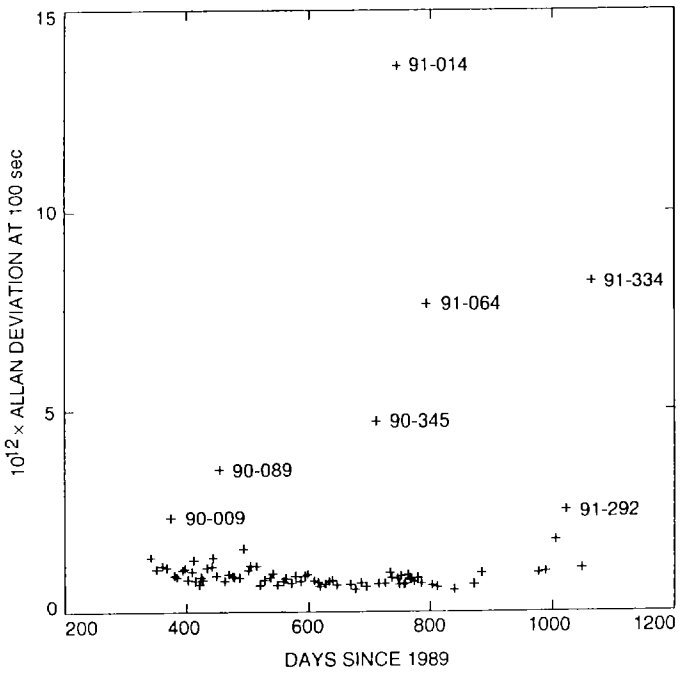

Fig. 16. Allan deviations at 100 sec for the 82 USO passes.

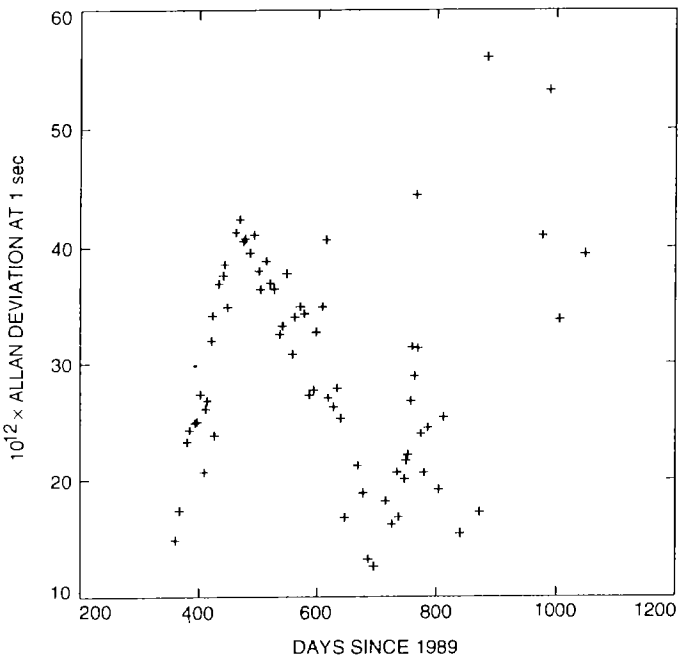

Fig. 18. Allan deviations at 1 sec for 73 USO passes (outliers identified in Figs. 14–17 have been removed).

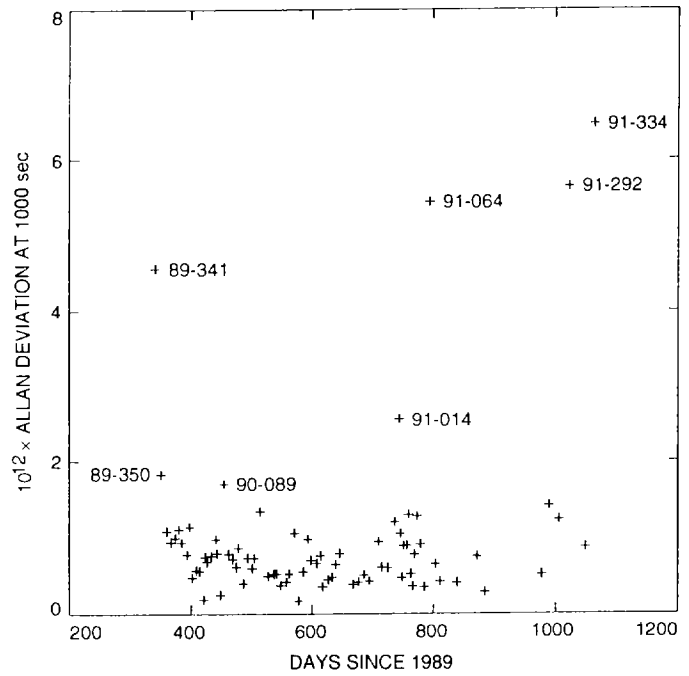

Fig. 17. Allan deviations at 1000 sec for the 79 USO passes.

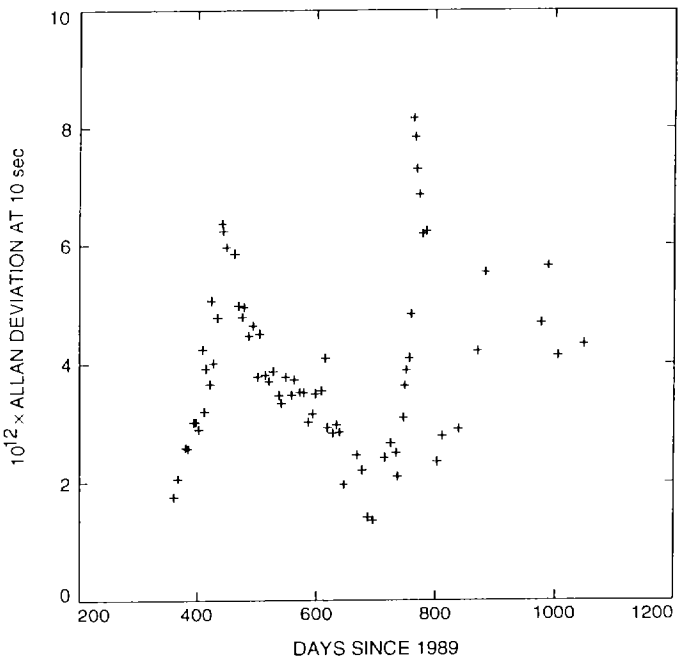

Fig. 19. Allan deviations at 10 sec for 73 USO passes (outliers identified in Figs. 14–17 have been removed).

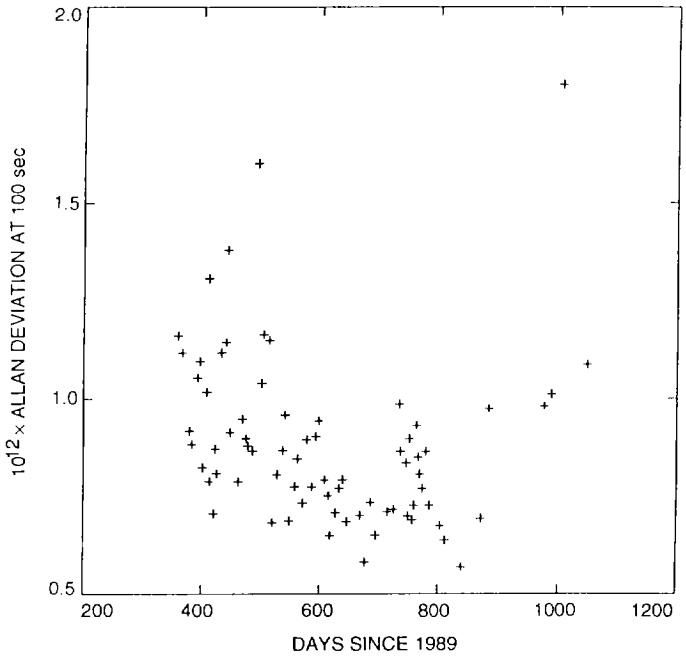

Fig. 20. Allan deviations at 100 sec for 73 USO passes (outliers identified in Figs. 14–17 have been removed).

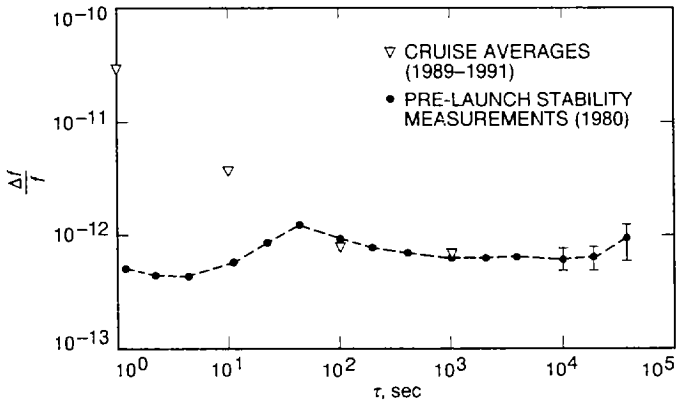

Fig. 22. In-flight USO-pass Allan-deviation measurement averages for 1, 10, 100 and 1000 sec superimposed with pre-flight Allan deviation measurements.

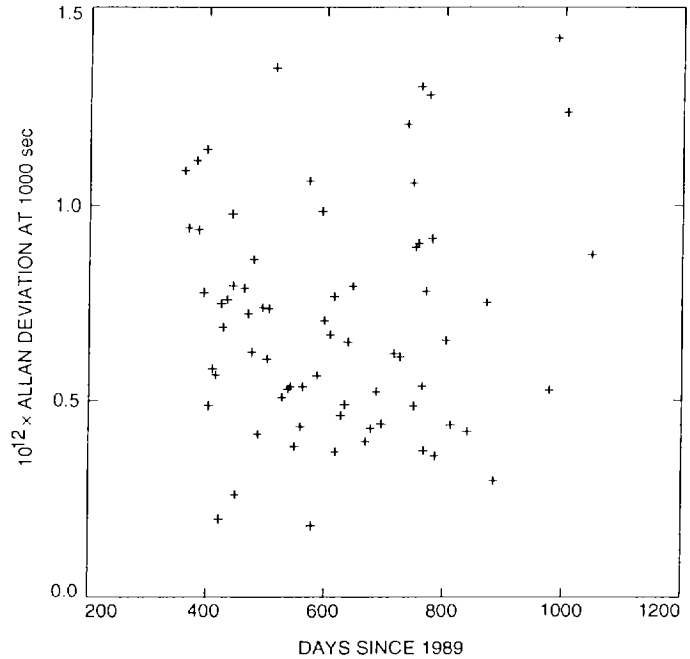

Fig. 21. Allan deviations at 1000 sec for 70 USO passes (outliers identified in Figs. 14–17 have been removed).

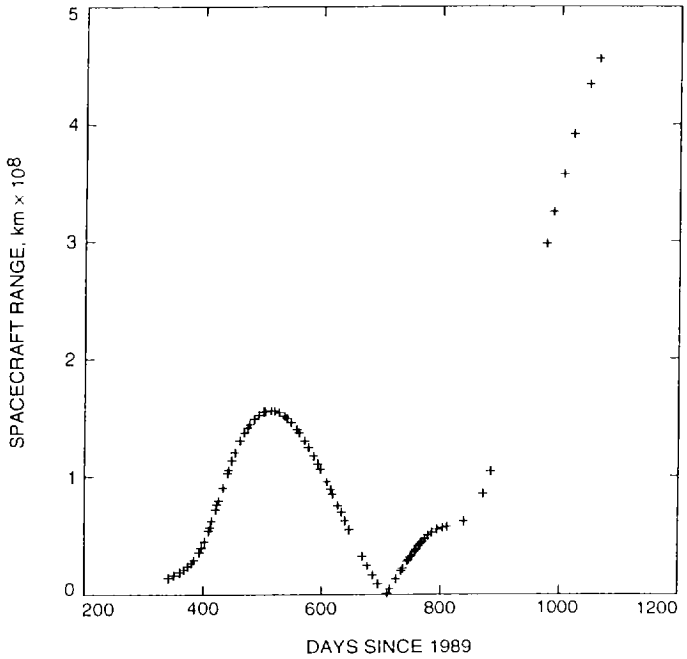

Fig. 23. Spacecraft range for each USO pass. Launch occurred at day 291; the dip at 707 days after 1989.0 was the Earth 1 flyby.

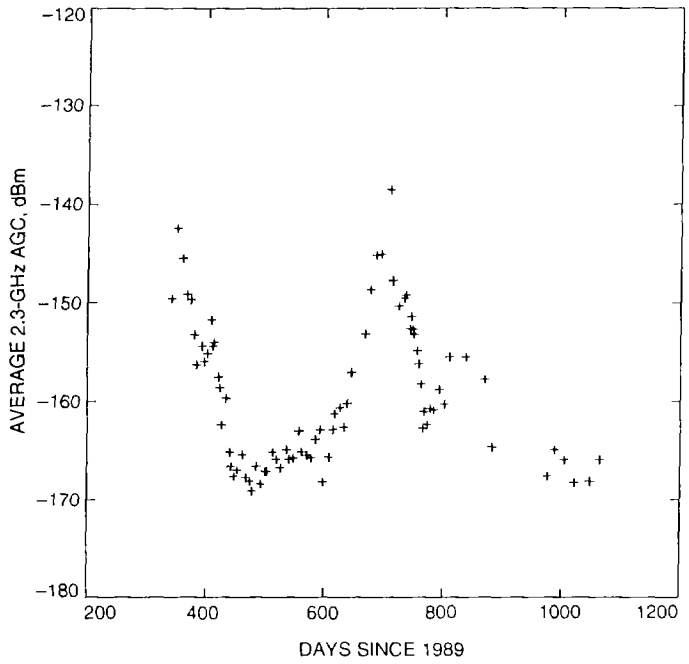

Fig. 24. Signal strength (AGC level) measured for each USO pass.

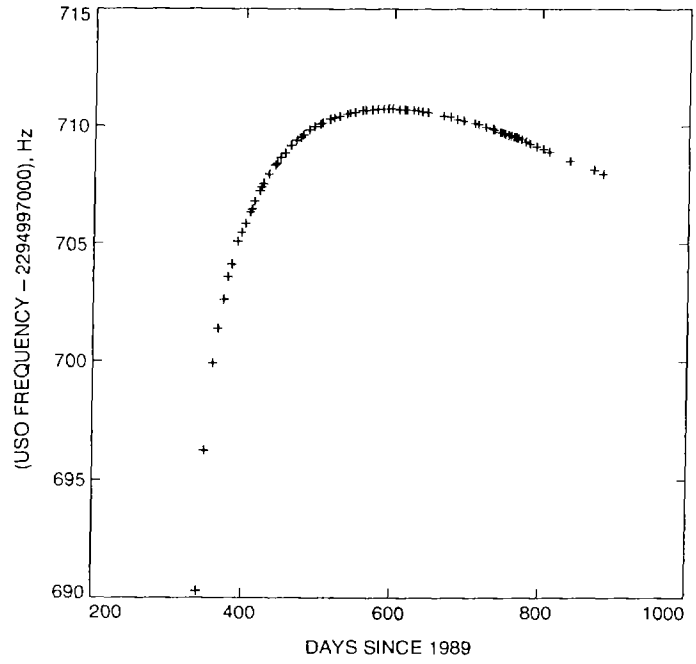

Fig. 26. Estimated spacecraft transmitted frequencies for 76 USO passes during the first USO on–off cycle after launch.

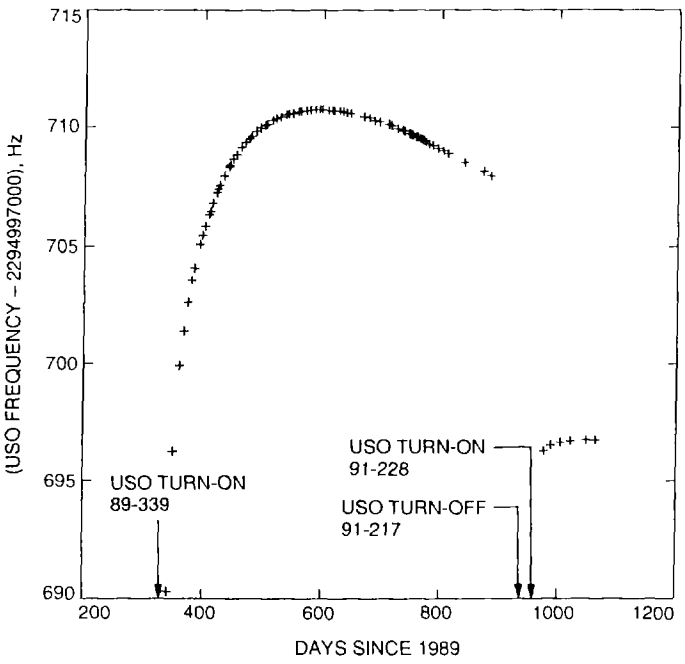

Fig. 25. Estimated spacecraft transmitted frequencies for all 82 USO passes as determined by STBLTY.

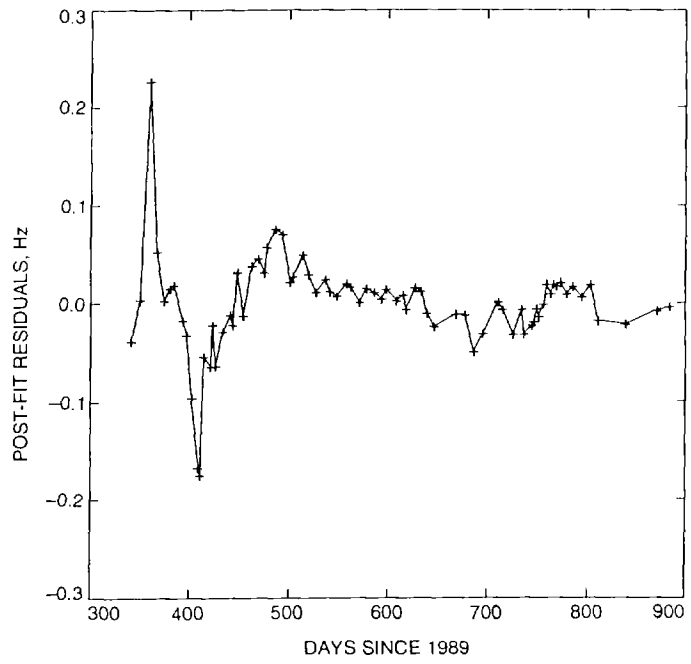

Fig. 27. Post-fit residuals of estimated spacecraft transmitted frequencies of Fig. 26 after fitting and removing an aging model.

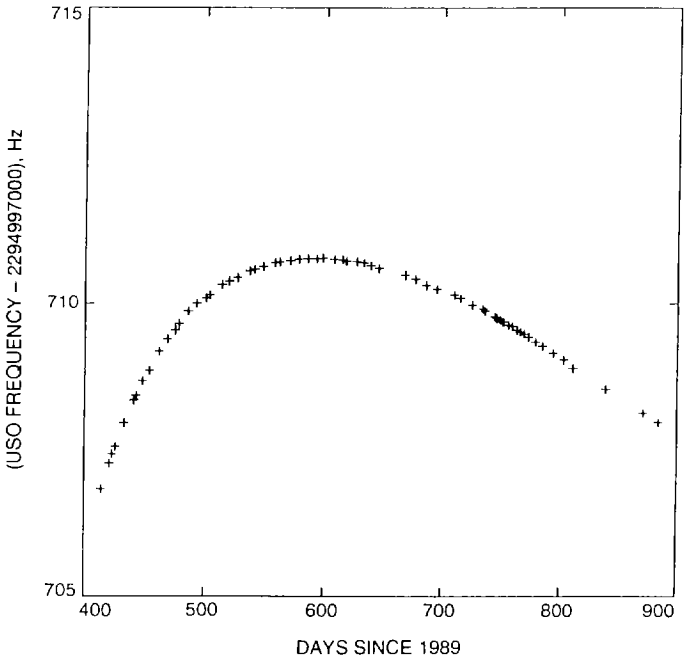

Fig. 28. Estimated spacecraft transmitted frequencies for 64 USO passes during the first USO on–off cycle after launch (the first 12 passes of Fig. 26 have been removed).

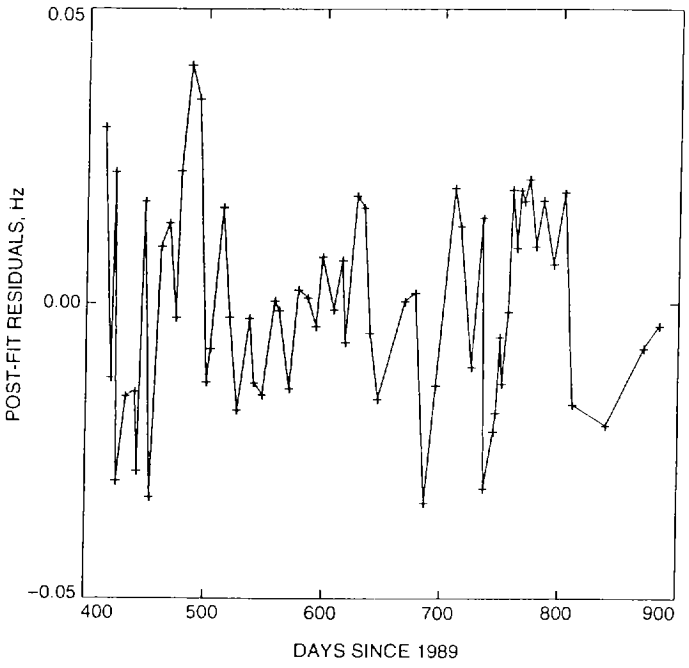

Fig. 29. Post-fit residuals of estimated spacecraft transmitted frequencies of Fig. 28 after fitting and removing an aging model.

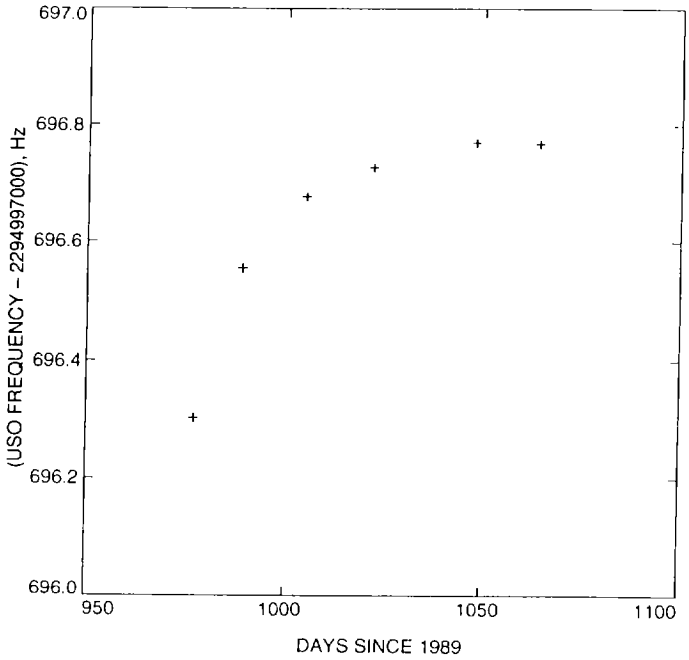

Fig. 30. Estimated spacecraft transmitted frequencies of 6 USO passes conducted after the first USO on–off cycle.